High Chalcocite Cu_2S: A Solid-Liquid Hybrid Phase

Lin-Wang Wang*

Material Science Division, Lawrence Berkeley National Laboratory, Berkeley, California 94720, USA

(Received 31 August 2011; published 24 February 2012)

There are materials that exist in unusual solid-liquid hybrid phases, for example, the superionics at high temperatures of 700 °C. Using *ab initio* molecular dynamics, we show that the intensely studied Cu_2S high chalcocite phase is actually a solid-liquid hybrid phase which exists in relatively low temperature (> 105 °C). Its formation mechanism is different from the superionics. We also show that the previously proposed atomic structure for high chalcocite is incorrect, and the low chalcocite to high chalcocite transition should be described as a sublattice solid to liquid transition.

DOI: 10.1103/PhysRevLett.108.085703 PACS numbers: 64.70.dj, 61.43.Bn, 61.50.Ks

Earthly materials usually exist in one of the three phases: solid, liquid, or gas. However, there are some exceptions. One example is the superionic phase of metal halogens like AgCl [1–4]. At high temperature (e.g,, 700 °C), the anion sublattice of these superions are melted as a liquid [1]. But the mechanical properties and shapes of the materials are controlled by the metal ion sublattices, which still have their solid forms. Studying such hybrid phase materials is quite interesting, especially for their potential applications. However, the superionic phase only exists in high temperature, which limits their applicability in practice. In this paper, we show that Cu_2S high chalcocite is such a hybrid phase with Cu ions diffusing like a liquid at a relatively low temperature of 105 °C. However, its formation mechanism is different from superionics, which makes it possible to exist at low temperatures and also qualifies it as a new phase. Our discovery overthrows a 50-year-old assumption that the high chalcocite is a solid solution with Cu atoms randomly occupying some given empty Wyckoff sites, but then frozen at those sites.

Copper sulfide is an important material intensively studied for its structural complexity and potential applications [5–7]. While $Cu_{2-x}S$ has many different phases, the stoichiometric compound Cu_2S (chalcocite) has three phases: the γ phase (for temperatures below 105 °C), the β phase (for temperatures between 105 °C and 425 °C), and α phase (for temperatures above 425 °C). The γ (low chalcocite: *L*-chalc.) to β (high chalcocite: *H*-chalc.) transition happens around the boiling temperature of water [6], which makes it challenging to be used in applications like solar cells, notwithstanding that it is an important solar cell material due to its ideal band gap of 1.2 eV and the ability to form good quality junctions like Cu_2S/CdS [8]. Cu_2S is a binary copper chalcogenide, which has more complicated counterparts like $CuCaF_2$, $CuInSe_2$, and $CuIn(GaSe)_2$; all are important solar cell compounds [9].

The crystal structures of low and high chalcocites have been studied extensively for more than 50 years using x-ray diffraction (XRD) data [10–12]. Despite some initial controversies [13,14], it has now been widely accepted that the *H*-chalc. has a $P6_3/mmc$ hexagonal symmetry crystal structure with two molecule units $(Cu_2S)_2$ per unit cell [10]. While the S atoms occupying a hexagonal lattice, the Cu atoms randomly occupy a few possible high symmetry Wyckoff sites with certain probabilities, and each Cu atom is fixed at its position as in a solid. This is thus a solid-solution (alloy) picture for the Cu sublattice. In contrast, the *L*-chalc. has a large orthorhombic unit cell with 96 molecule units $(Cu_2S)_{96}$, but each Cu atom has a unique site [11,12]. Thus the *L*-chalc. to *H*-chalc. phase transition is believed to be a crystal to solid alloy transition.

In this study, via large scale *ab initio* molecular dynamics (MD) simulations, we show that the *H*-chalc. phase should be more properly described as a solid-liquid hybrid phase, while the S atoms maintain an approximate hexagonal crystal structure, the Cu atoms randomly diffuse between different sites with a self-diffusion coefficient similar to that of a liquid. Furthermore, the averaged Cu position is not at the previously proposed high symmetry sites. Rather, it is at the sites similar to the *L*-chalc. case. This solid-liquid hybrid phase is similar to the superionic phase of metal halogens like AgCl, AlBr, AgI, CaF_2, CaF_2 [1–4]. While the superionic phase of the metal halogens is often characterized by a significant increase of Frenkel defect (vacancy and interstitial atoms) at high temperature (> 700 °C) which facilitates the ion diffusion [3,4], in *H*-chalc., the melting of the Cu sublattice is not accompanied by the increase of such defect sites. Since there are already more possible occupation sites than the number of Cu atoms, such increase of defect is not necessary. This is the reason why the liquid Cu *H*-chalc. can exist at relatively low temperature and has a different temperature dependence of its ion mobility [3,15].

The calculations are carried out using Vienna *ab initio* simulation package (VASP) [16] with the projector-augmented-wave method [17] using generalized gradient approximation [18] for the exchange-correlation energy in the density functional theory (DFT) formalism. A 500 eV cutoff energy is chosen for the plane-wave basis, and the Cu *s*, *d*, S *s*, *p* electrons are included as the valence

electron in the calculation. A $2 \times 2 \times 2$ Monkhorst-Pack k-point set with shift (no Γ point) is used. Molecular dynamics is carried out using Born-Oppenheimer ground states with 2 fs as the time step. A thermostat is used to control the temperature. Most of the calculations have been carried out on the supercomputer: Intrepid at Argonne Leadership Computer Facility using 2048 cores.

The L-chalc. has an orthorhombic unit cell with 96 f.u. [$(Cu_2S)_{96}$] [19]. However, the orthorhombic cell can be approximately divided into two identical monoclinic cells $Cu_{96}S_{48}$ with only small modifications. This 144 atom supercell has been used in previous theoretical studies [8,20], and it will also be used here. In both L-chalc. and H-chalc., the S atoms form an approximate c axis slightly elongated hexagonal close packed (EHCP) lattice with A-B-A-B stacking as shown in Fig. 1 [11]. In the L-chalc., the Cu atoms can be classified into three equal size groups occupying a, d, e sites in Fig. 1 [19], all have threefold coordinates. We have taken the experimentally determined L-chalc. atomic positions [19], and did an atomic relaxation according the DFT total energy at zero temperature. The DFT relaxed structure deviates only 0.24 Å per atom from the original structure. Thus the proposed L-chalc. is stable. The electronic structure of such L-chalc. has been calculated previously under DFT with an additional Cu s state shift derived from smaller system GW calculations [20], and the obtained band gap of 0.6 eV is lower than the experimentally observed value of 1.2 eV. In our DFT calculation, the band gap at the Γ point for L-chalc. is only 0.36 eV. With the $2 \times 2 \times 2$ k-point grid without the Γ point, there is always a finite band gap during our MD simulations described below.

We next calculated the H-chalc. structure. According to previous XRD fitting [10], in H-chalc. the S atoms occupy an EHCP sublattice, while the Cu atoms randomly distributed into the a, b, c sites (with three-, four- and twofold coordinates) shown in Fig. 1 with probabilities of 31%, 41%, and 28% respectively [10]. After averaging over Cu distributions, the high symmetry H-chalc. has a small hexagonal unit cell of two Cu_2S molecule units (with $a = 3.89$ Å, $c = 6.88$ Å, and $c/a = 1.77$, slightly elongated from the ideal HCP value of 1.633). To construct a random distribution of Cu, we have followed a previous theoretical work [20], using a $2 \times 2 \times 2$ supercell of the primary unit cell, and with a weighted random number to generate the Cu occupation. We will call this $Cu_{32}S_{16}$ system the "unrelaxed H-chalc. model" (UHCM). We have first relaxed its atomic structure following the DFT energy and found that the 4 and 2 coordinated Cu atoms (b and c in Fig. 1) have relaxed into nearby 3 coordinated sites (either d or e). This is the first indication that the proposed H-chalc. structure is unstable, at least at zero temperature. We have also taken the L-chalc. structure, and displaced one Cu atom from d (or e) sites into a nearby b or c sites, then relax the structure. Once again, we found that the Cu atom relaxes to the original d (or e) sites, and there is no potential barrier between the b and c sites to the d and e sites. The b and c sites are simply unstable at zero temperature.

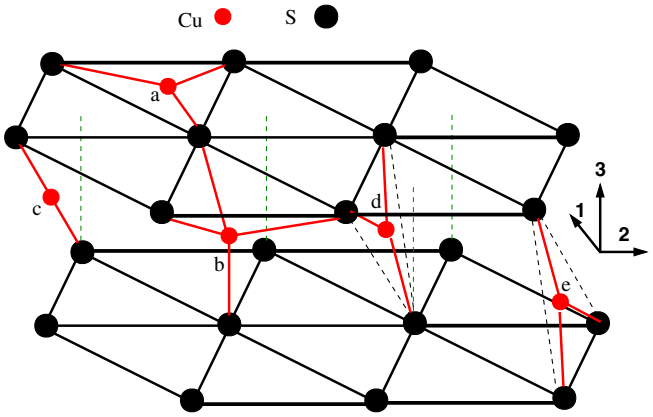

FIG. 1 (color online). Schematic view of the Cu_2S structure.

We next carried out long time *ab initio* Born-Oppenheimer molecular dynamics simulations. We are mostly interested in the atomic structure of L-chalc. and H-chalc., instead of the phase transition between them since our simulation time is not long enough to capture the phase transition properties (e.g., the hysteresis, and the specific heat change during the transition). Thus we have chosen 290 K as our temperature for L-chalc. and 450 K as our temperature for H-chalc. We have used the same 144 atom cell as our simulation cell for both L-chalc. and H-chalc. phases, because their unit cells are commensurate with each other as shown in Ref. [11].

The L-chalc. has been simulated for 6 ps, while the H-chalc. has been simulated for 12 ps. The average distance square of S and Cu atoms from their $t = 0$ positions as functions of time are shown in Fig. 2. We can see that, for the L-chalc. the average distances do not grow with time, indicating both the S and Cu atoms do not diffuse. In contrast, the average distance square for Cu in H-chalc. grows linearly with time t, following a typical random diffusion picture. Further analysis shows that, the diffusions along the directions 1 and 2 (defined in Fig. 1) are about twice as much as diffusions along the direction 3 (see Fig. 1S in the Supplementary Material [21]), and most of the diffusion comes from the Cu atoms between the S planes (see Fig. 2S). Figure 3(a) shows the Cu atom which diffuses the longest distance in our simulation. It certainly hopped several times from one sites to another. From the slope of the $d^2(t)$ curve, we yield an averaged Cu diffusion constant of 3.2×10^{-6} cm^2 s^{-1}. The Cu diffusion in chalcocites has been studied experimentally since 60 years ago [15,22–24]. It can be measured either as part of the electric conductivity [15,23], or from the copper precipitation on the electrode [22,24]. The copper precipitation is a direct measurement of copper diffusion, its

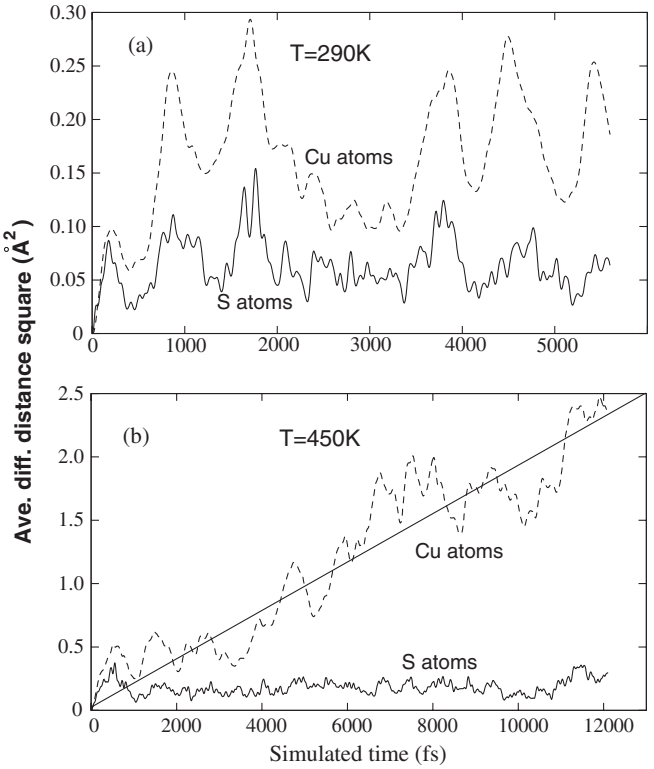

FIG. 2. Average diffusion distance squares as functions of time t, for the L-chalc. 290 K temperature simulation (a), and H-chalc. 450 K simulation (b).

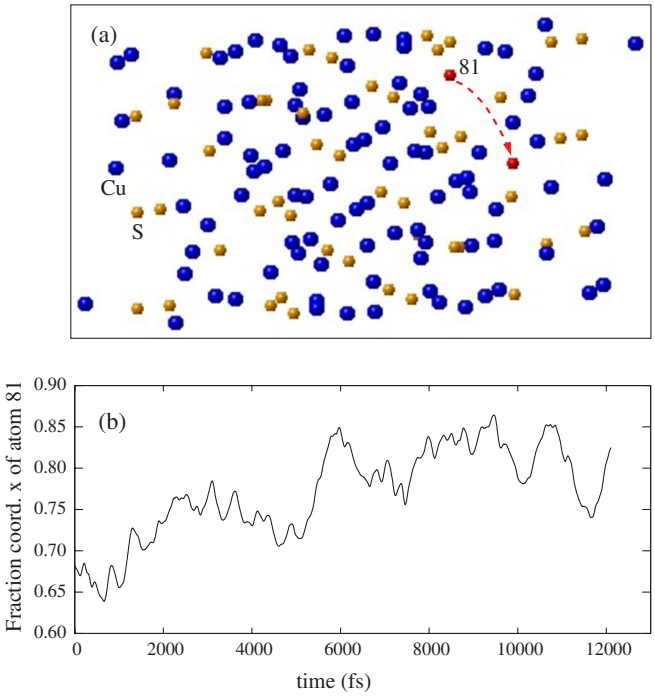

FIG. 3 (color online). (a) Simulated cell with an S atom denoted by yellow ball, Cu by blue ball, and the longest diffusion Cu atom (atom 81) by red ball. Its initial and final positions are connected by a dashed line, (b) the fractional coordinate x (which in the direction 1 of Fig. 1) of atom 81 as a function of time t.

measured $n_d D$ at 450 K is 10^{17} cm^{-1} s^{-1}, where n_d is supposedly the defect (Cu vacancy) density. The picture in Ref. [22] was that the Cu diffusion is proportional to Cu vacancy as in a traditional atomic diffusion picture in a crystal. However, the measured $n_d D$ are the same even though several samples with different n_d are used [22]. In our current picture, the Cu atoms are diffusing without the help of vacancy, thus we should use the total density of Cu to replace n_d. This will give us $D = 2.2 \times 10^{-6}$ cm^{-2} s^{-1}, which is rather close to our calculated result.

Note that, this Cu self-diffusion coefficient is only 5 to 10 times smaller than typical simple liquid self-diffusion constants, e.g., 1.6×10^{-5} cm^{-2} s^{-1} in Argon, 2.2×10^{-5} cm^{-2} s^{-1} in water, and larger than the values in some of the organic solvents [25]. The Cu trajectory in Fig. 3(b) shows that the Cu atom diffuses continuously from one site to another much like in a liquid. However, it is well known that the Cu diffusion barrier can be small in chalcogenides [20]. It is thus worth to investigate this further from the potential landscape of the system. We have first calculated the potential barrier between the relaxed L-chalc. structure and a structure with one Cu displaced from site d or e (Fig. 1) to a nearby three S triangle center. Such Cu displaced structures are not always stable (e.g., they can relax back to the original L-chalc). In the stable cases, they can have very small ($\sim$ 10 meV) barrier (see Fig. 3S). Second, we have calculated the potentials along the MD trajectory path. We find multiple potential minima along the path (see Fig. 4S), and the potential barrier between the nearby minima can also be small ($\sim$ 50 meV) (see Fig. 5S), in the same order as the kT. More importantly, the atomic movement from one minimum to a nearby minimum (e.g., for Fig. 5S) can involve similar magnitude displacements from several Cu atoms, not just one. All these fit better in the picture of a typical liquid, rather than the picture of single Cu atom hopping. Thus, overall, the Cu sublattice should be more appropriately described as a liquid phase, with the L-chalc. to H-chalc. transition as a solid to liquid phase transition for its Cu sublattice. This is like the superionic case where one sublattice is melt [1,2]. One difference is that in superionic case, the diffusion of the melt sublattice depends on creation of Frenkel defect [3]. In H-chalc. such point defect is not necessary due to the preexistence of the vacant sits (not all the a, d, e sites are occupied).

We next like to know, whether the Cu will occupy sites b and c, instead of d and e, in H-chalc. during the MD. To check this, for each Cu atom, we have found its 2, 3, and 4 closest S atoms, and calculated the center points of these 2, 3, and 4S atom clusters. We then calculated the distance between the Cu atom and the corresponding 2S, 3S, and 4S center points. The distant distributions for 290, 450 K MD simulations, the zero temperature relaxed

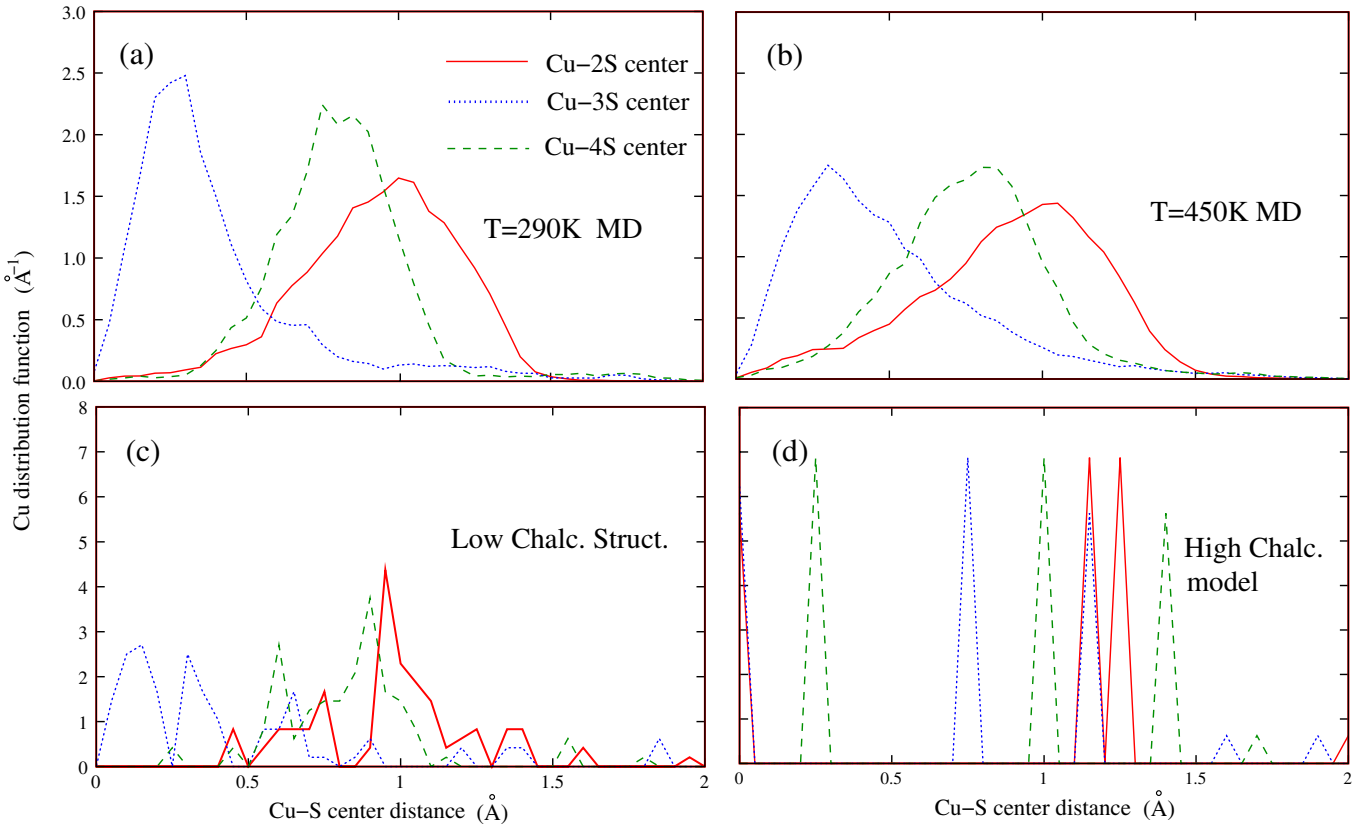

FIG. 4 (color online). Distance distribution function of Cu atoms to the centers of 2S, 3S, and 4S atoms for different structures and simulated systems. The high Chalc. model in (d) is the UHCM discussed in the text, while the low Chalc. structure in (c) is the DFT relaxed structure.

L-chalc. structure, and the UHCM are shown in Fig. 4. The 290 K MD and the relaxed *L*-chalc. structure have qualitatively similar distribution functions, albeit the MD results are smoothed by temperature effect. The closest site from Cu is the 3S center (*a*, *d*, *e* sites in Fig. 1). The situation for the 450 K MD result is similar to the 290 K MD. The closest site is also the 3S site, although the distribution is broaden due to larger oscillation and diffusion of the Cu atoms. In contrast, for the UHCM (where the Cu atoms occupying *a*, *b*, *c* sites), there is a peak for each of the 2S, 3S, and 4S curves within 0.25 Å distance from the origin. Thus, the 450 K situation is more close to 290 K case, than the UHCM case. In other words, during the MD, the Cu atoms will spend most time near *a*, *d*, *e* sites, instead of the assumed *a*, *b*, *c* sites [10]. This is further supported by the calculated Cu-Cu, Cu-S, S-S correlation functions (see Fig. 6s).

We next study the TEM image and XRD data fitting of the *H*-chalc. structure. While we will focus on the TEM images, the XRD data can also be used to construct electron charge density which looks rather similar to the TEM image [10,26]. Thus similar conclusion can be made for the XRD fitting. Using all the MD time steps, one can construct an approximate TEM image (see the supplementary material [21]). The simulated TEM image viewing from the direction 2 (Fig. 1) for 290 K MD is shown in Fig. 5(a) in comparison with the experimental TEM image taken from Ref. [27]. More interesting is the simulated 450 K MD TEM image shown in Fig. 5(d) constructed from the atomic trajectories in our simulation. It is significantly different from Fig. 5(a), showing more symmetry and pattern. Nevertheless, it is not completely symmetric. This is due to our limited simulated time, 12 ps, which is not long enough for the system to show the complete symmetry. However, due to the diffusion shown in Fig. 2 and 3, it is reasonable to assume that after a much longer simulation time, the averaged system will be symmetric (note, this will not be true for the 290 K case due to the lack of diffusion). As a result, we can symmetrize Fig. 5(d) according to the $P6_3/mmc$ space group [10] and yield Fig. 5(e), which is very close to the experimental TEM image of Fig. 5(f) [27]. One can also construct the TEM image using the UHCM. This time, to yield the full symmetry, all the *a*, *b*, *c* sites are occupied with Cu but with weights corresponding to a 0.31:0.41:0.28 ratio. The so constructed TEM image is shown in Fig. 5(c), which is sharper than the 450 K MD ones, but still similar to the experimental image in Fig. 5(f). All these indicate that, our simulated 450 K MD structure is consistent with the experimental TEM data (likely also with the XRD data

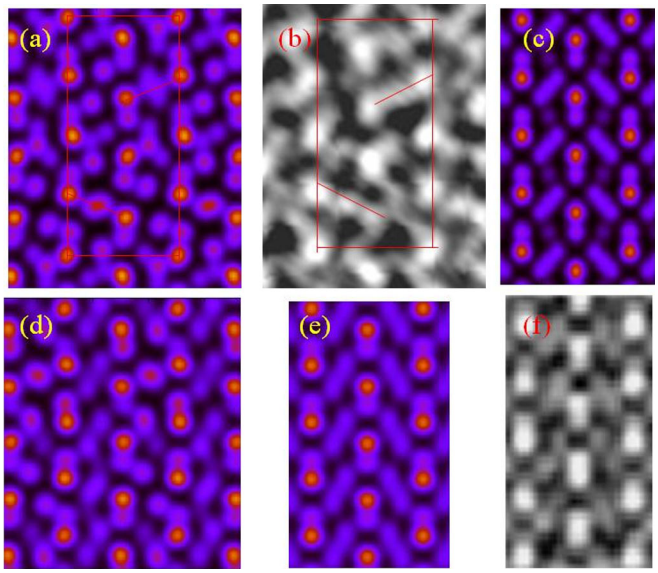

FIG. 5 (color online). (a) Simulated TEM image for 295 K MD; (b) the experimental *L*-chalc. TEM image take from Ref. [27], (c) the constructed TEM image from the unrelaxed *H*-chalc. model, (d) the simulated TEM image for 450 K MD, (e) the symmetrized 450 K MD image from image (d), (f) the experimental TEM image take from Ref. [27]. The horizontal axis is the direction 3 shown in Fig. 1, while the vertical axis is the direction 1. The viewing directions of these images are from direction 2 shown in Fig. 1. The bright red spots are S atoms. From red to blue, the density decreases.

judged from the XRD constructed electron charge density [10,26]), but at the same time, such data is not enough to uniquely determine the crystal structure [e.g. distinguish between Fig. 5(e) from Fig. 5(c)]. Indeed, in the original work of the XRD fitting [10,26], there were discussions about the relatively large fitting errors in the proposed *H*-chalc. structure.

In summary, using large scale *ab initio* MD simulations, we have revealed that the *H*-chalc. is a solid-liquid hybrid phase, with Cu atoms located near the *a*, *d* and *e* sites, instead of the *a*, *b* and *c* sites as previously assumed. More importantly, the *H*-chalc. is not a fixed solid-solution phase, instead its Cu sublattice is in liquid phase while the S sublattice is in solid crystal phase. The *L*-chalc. to *H*-chalc. phase transition is a sublattice solid to liquid transition. This is the first time such low temperature solid-liquid hybrid phase has been found (in a well known material). This discovery also makes it worthwhile to reevaluate many similar solid-solutions with empty sites partially occupied.

We like to thank Dr. Lukashev for providing the high chalcocite model structure atomic coordinates, Dr. H. M. Zheng and Dr. P. Alivisatos for stimulating discussions. This work is supported by SC/BES/MSED of the U.S. Department of Energy under the Contract No. DE-AC02-05CH11231. Under the Department of Energy's Innovative and Novel Computational Impact on Theory and Experiment (INCITE) program, it used the resources of the Argonne Leadership Computing Facility at Argonne National Laboratory. It also uses the resources of the National Energy Scientific Computing Center at Lawrence Berkeley National Laboratory.

*lwwang@lbl.gov

[1] J. P. Boilot, Ph. Colomban, and R. Collonguess, Phys. Rev. Lett. **42**, 785 (1979).
[2] N. Hainovsky and J. Maier, Solid State Ionics **76**, 199 (1995).
[3] N. Hainovsky and J. Maier, Phys. Rev. B **51**, 15789 (1995).
[4] A. Dent, P. A. Madden, and M. Wilson, Solid State Ionics **167**, 73 (2004).
[5] H. T. Evans, Jr., Am. Mineral. **66**, 807 (1981).
[6] D. J. Chakrabarti and D. E. Laughlin, Bull. Alloy Phase Diagrams **4**, 254 (1983).
[7] M. Posfal and P. R. Buseck, Am. Mineral. **79**, 308 (1994).
[8] B. Sadtler, D. O. Demchenko, H. Zheng, S. M. Hughes, M. G. Merkle, U. Dahmen, L. W. Wang, and A. P. Alivisatos, J. Am. Chem. Soc. **131**, 5285 (2009).
[9] N. Amin, J. Appl. Polym. Sci. **11**, 401 (2011).
[10] M. J. Buerger and B. J. Wuensch, Science **141**, 276 (1963).
[11] M. J. Wuensch and M. J. Buerger, Mineral Soc. Am., Special Paper, **1**, 164 (1963).
[12] H. T. Evans JR, Science **203**, 356 (1979).
[13] N. V. Belov and V. P. Butuzov, C.R. Acad. Sci. URSS **54**, 717 (1946).
[14] R. Ueda, J. Phys. Soc. Jpn. **4**, 287 (1949).
[15] Th. Pauporte and J. Vedel, Solid State Ionics **116**, 311 (1999).
[16] G. Kresse and J. Furthmuller, Phys. Rev. B **54**, 11169 (1996).
[17] G. Kresse and D. Joubert, Phys. Rev. B **59**, 1758 (1999).
[18] J. P. Perdew, K. Burke, and M. Ernzerhof, Phys. Rev. Lett. **77**, 3865 (1996).
[19] H. T. Evans JR., Z. Kristallogr. **150**, 299 (1979).
[20] P. Lukashev, W. R. L. Lambrecht, T. Kotani, and M. van Schilfgaarde, Phys. Rev. B **76**, 195202 (2007).
[21] See Supplemental Material at http://link.aps.org/supplemental/10.1103/PhysRevLett.108.085703 for details.
[22] S. Y. Miyatani and Y. Suzuki, J. Phys. Soc. Jpn. **8**, 680 (1953).
[23] A. Hulanicki and A. Lawenstam, Talanta **23**, 661 (1976).
[24] E. Hirahara, J. Phys. Soc. Jpn. **6**, 422 (1951); **6**, 428 (1951).
[25] H. O. Phillips, A. J. Shor, A. E. Marcinkowsky, and K. A. Kraus, J. Phys. Chem. **81**, 682 (1977).
[26] B. Sadanaga, M. Ohmasa, and N. Morimoto, Mineralogical Journal **4**, 275 (1965).
[27] H. Zheng, J. B. Rivest, T. Miller, B Sadtler, A. Lindenberg, L. W. Wang, C. Kisielowski, and A. P. Alivisatos, Science **333**, 206 (2011).